Nowcasting of Precipitation Over the Indian Region Using INSAT-3D Outbound Longwave Radiation Data

Introduction

Nowcasting was first defined by Keith Browning in 1981 as “the description of the current state of the weather in detail and the prediction of changes that can be expected on a timescale of a few hours” (Schmid et al.). Precipitation nowcasting refers to the forecasting rainfall intensity over such a small time period. In our study, the nowcasting is done with the help of Outbound Longwave Radiation (OLR) data from the INSAT-3D satellite which used the IMAGER sensor (Singh). Our area of study spanned the domain 0N – 40N, 60E – 100E, centered around the Indian subcontinent. Lead time of the nowcast is 1 – 3 hours, with predictions being made for the next 3 hours.

Methodology

The paper uses sparse optical flow across OLR data to extrapolate the predictions. “OLR is considered as a proxy for the deep convection and used as a heuristic indicator of cloudiness or for precipitation estimation” (Liang, chap.5). `3DIMG_L2B_OLR` dataset geo-locates every pixel, allowing us to build motion vectors for each pixel to extrapolate the movement of clouds using the value of OLR (W/m^2) data per pixel. Optical flow extrapolation operates under the assumption that motion vectors remain constant from the final input image (at time t) until the extent of the nowcasting (at time t+6). Dataset provided has images taken at half-hour time steps. Predicted images were verified using true OLR images garnered from the dataset; the metric used was fractional skills score (FSS), which allows us to “measure how forecast skill varies with spatial scale” (Roberts and Lean). Moreover, one could validate the forecasts using INSAT-3D Hydro Estimator precipitation estimates (Varma) to validate the precipitation

nowcasts; this will be done and published in future work due to time and computational constraints.

The optical flow method used is the local Lucas-Kanade method, the pySTEPS library (Pulkkinen et al.) uses the OpenCV implementation of the method. The key features were detected using blob feature detection methods (Lindeberg). The sparse motion fields generated are interpolated using radial basis function (RBF) interpolation (Franke) to return a dense motion field.

Below is the source code:

```
flow_params = {
    'dense': True,
    'fd_method': 'blob',
    'interp_method': 'rbfinterp2d'
}

extrapolate_params = {
    'timesteps': 6,
    'interp_order': 3,
    'return_displacement': False,
}

all_frames_gen_array = []
all_frames_truth_array = []
for i in range(6, none_idx-6):
    motion_field = dense_lucaskanade(input_img[i-6:i],
                                     **flow_params)
    extrapolated_frames = extrapolate(input_img[i-1], motion_field,
                                      **extrapolate_params)
    all_frames_gen_array.append(extrapolated_frames)
    all_frames_truth_array.append(input_img[i:i+6])
```

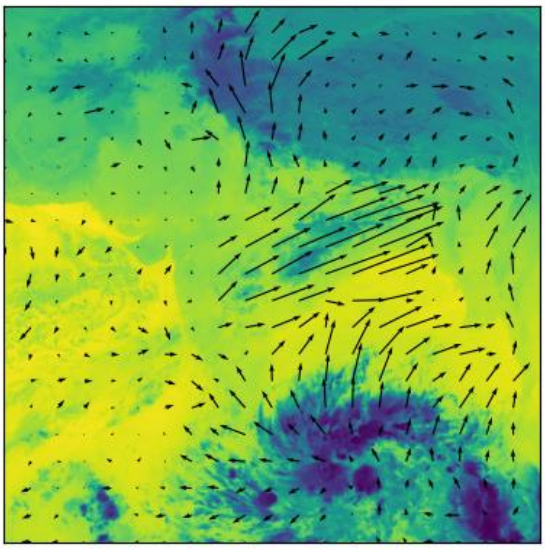

Figure 1: Motion field generated from 't-6' to 't-1' @ 't = 6'

Figure 1 is the vector plot of one of the motion fields generated from the above code snippet.

Dataset provided by MOSDAC has been processed at the L2B level; the only pre-processing that was performed was the windowing of data from 't-6' to 't+5' for every available 't.' Windows with missing data were skipped. Values of OLR data ranged between 120 and 280 W/m^2 for the data that was used. Timeframe of the data used ranges from 10th January, 2022, 00:00 till 13th January, 2022, 08:00. A total of 161 windows were formed and worked upon. The source code for the above is available at the online repository linked in the appendix.

Metrics

Mean FSS for all the windows was 0.994. The metric conceals a clear degradation of the nowcast image as the lead time increases. The RMSE score for prediction at 't' averaged 8.93, while the average of the predicted image at 't+5' was 21.91.

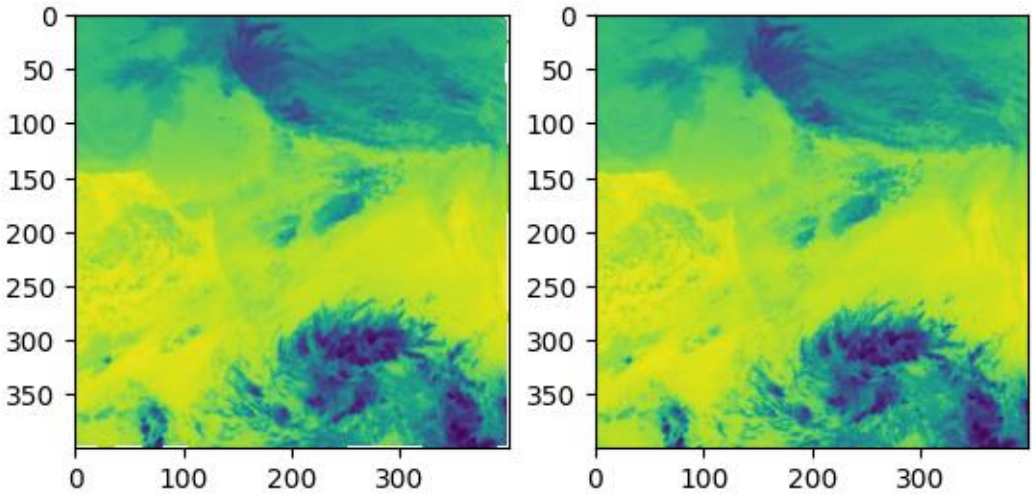

Figure 2: Plot on the left is the predicted image, plot on the right is the true image.

One frame of the prediction is outlined in figure 2. Both of them are plots at 't = 6.' This is the best-case scenario as we are comparing the immediate extrapolated frame from the input window. Moreover, the blobs that are present on the image are distinct and well-defined.

Earlier Techniques

Ensemble forecasting is the method used within numerical weather prediction to nowcast precipitation, instead of machine learning techniques such as optical flow or generative neural networks. Ensemble forecasting is a form of Monte Carlo analysis. Multiple simulations are conducted using differing starting conditions to account for uncertainty in forecast models (Manousos). The errors can be introduced by imperfect input data, which is further amplified by the chaotic nature of weather systems. Errors could also be introduced during model formations.

Numerical weather prediction is quickly being surpassed by ML and DL techniques, one driving factor is the increased availability of data that allows for sufficient training of the neural networks. This shift allows forecasting and nowcasting models to be self-consistent in their forecasts from the ground up, even during changes in the input data (Schultz, M. G., et al.).

Ensemble techniques can and should be used to improve machine learning workflows. One improvement that can be made to the method outlined above is to generate multiple motion fields using the input window i.e., 't-6 to t-1', 't-4 to t-1' and, 't-2 to t.-2' A KNN model can be trained to pick out the motion field that best correlates with the field generated by the images in the window 't to t+5.' This will allow us to extrapolate new frames using the most ideal motion field calculated using optical flow techniques.

Conclusion

There are inherent limitations to nowcasting using optical flow techniques, the obvious one is the one-dimensionality of the data that is being used to extrapolate frames. Spatio-temporal features are included during the creation of motion fields but it only takes OLR data into account, if one would have more data available, there would be no easy way for us to include them in the generation of the optical flow. Building upon this fact, and reading available literature (Marrocu and Massidda), the most accurate nowcasts are performed using generative neural networks, ideally a neural network that takes temporal aspects into account. A model that is widely used for precipitation nowcasting is the Convolutional LSTM model, the model is trained on RADAR images to perform precipitation nowcasting (Shi et al.); doing the same for OLR data will be interesting and something that might be worked on and showcased in a future paper.

Appendix

GitHub repository for source code and visualisation:

https://github.com/jeetsh4h/Nowcasting-OLR-Optical-Flow

References

Franke, Richard. “Scattered Data Interpolation: Tests of Some Methods.” Mathematics of Computation, vol. 38, no. 157, 1982, pp. 181–200. DOI.org (Crossref), https://doi.org/10.1090/S0025-5718-1982-0637296-4.

Liang, Shunlin, editor. Comprehensive Remote Sensing. Elsevier, 2018.

Lindeberg, Tony. “Scale Selection Properties of Generalized Scale-Space Interest Point Detectors.” Journal of Mathematical Imaging and Vision, vol. 46, no. 2, June 2013, pp. 177–210. Springer Link, https://doi.org/10.1007/s10851-012-0378-3.

Manousos, Peter. "Ensemble Prediction Systems". Hydrometeorological Prediction Center. Retrieved 2010-12-31.

Marrocu, Marino, and Luca Massidda. “Performance Comparison between Deep Learning and Optical Flow-Based Techniques for Nowcast Precipitation from Radar Images.” Forecasting, vol. 2, no. 2, June 2020, pp. 194–210. www.mdpi.com, https://doi.org/10.3390/forecast2020011.

Pulkkinen, Seppo, et al. “Pysteps: An Open-Source Python Library for Probabilistic Precipitation Nowcasting (v1.0).” Geoscientific Model Development, vol. 12, no. 10, Oct. 2019, pp. 4185–219. DOI.org (Crossref), https://doi.org/10.5194/gmd-12-4185-2019.

Roberts, Nigel M., and Humphrey W. Lean. “Scale-Selective Verification of Rainfall Accumulations from High-Resolution Forecasts of Convective Events.” Monthly Weather Review, vol. 136, no. 1, Jan. 2008, pp. 78–97. DOI.org (Crossref), https://doi.org/10.1175/2007MWR2123.1.

Schmid, Franziska, et al. Nowcasting Guidelines – A Summary. 27 Nov. 2019, https://public.wmo.int/en/resources/bulletin/nowcasting-guidelines-%E2%80%93-summary.

Schultz, M. G., et al. “Can Deep Learning Beat Numerical Weather Prediction?” Philosophical Transactions of the Royal Society A: Mathematical, Physical and Engineering Sciences, vol. 379, no. 2194, Apr. 2021, p. 20200097. DOI.org (Crossref), https://doi.org/10.1098/rsta.2020.0097.

Shi, Xingjian, et al. "Deep learning for precipitation nowcasting: A benchmark and a new model." *Advances in neural information processing systems* 30 (2017)

Singh, Randhir. INSAT-3D IMAGER L2B OUTGOING LONGWAVE RADIATION PRODUCT. Meteorological and Oceanographic Satellite Data Archival Centre. DOI.org (Crossref), https://doi.org/10.19038/SAC/10/3DIMG_L2B_OLR. Accessed 23 Apr. 2023.

Varma, A. K. INSAT-3D IMAGER L2B HYDRO ESTIMATOR PRODUCT. Meteorological and Oceanographic Satellite Data Archival Centre. DOI.org (Crossref), https://doi.org/10.19038/SAC/10/3DIMG_L2B_HEM. Accessed 23 Apr. 2023.

Contributions

Jeet Shah: Worked on the implementation of the optical flow algorithm and found the algorithms that must be used in the given scenario. Worked on visualisation of the model and its outputs.

Archit Murali: Worked on pre-processing of data i.e., windowing and error handling when a frame is unavailable.